Lightning NO_x Emissions: Reconciling Measured and Modeled Estimates With Updated NO_x Chemistry

B. A. Nault[1,2] (iD), J. L. Laughner[3] (iD), P. J. Wooldridge[3], J. D. Crounse[4] (iD), J. Dibb[5] (iD), G. Diskin[6] (iD), J. Peischl[7,8] (iD), J. R. Podolske[9], I. B. Pollack[7,8,10] (iD), T. B. Ryerson[7] (iD), E. Scheuer[5], P. O. Wennberg[4,11] (iD), and R. C. Cohen[1,3] (iD)

[1]Department of Earth and Planetary Science, University of California, Berkeley, CA, USA, [2]Now at Cooperative Institute for Research in the Environmental Sciences and Department of Chemistry, University of Colorado Boulder, Boulder, CO, USA, [3]Department of Chemistry, University of California, Berkeley, CA, USA, [4]Division of Geological and Planetary Sciences, California Institute of Technology, Pasadena, CA, USA, [5]Earth Systems Research Center, Institute for the Study of Earth Oceans and Space, University of New Hampshire, Durham, NH, USA, [6]NASA Langley Research Center, Hampton, VA, USA, [7]Chemical Sciences Division, Earth System Research Lab, National Oceanic and Atmospheric Administration, Boulder, CO, USA, [8]Cooperative Institute for Research in the Environmental Sciences, University of Colorado Boulder, Boulder, CO, USA, [9]NASA Ames Research Center, Mountain View, CA, USA, [10]Now at Atmospheric Science Department, Colorado State University, Fort Collins, CO, USA, [11]Division of Engineering and Applied Science, California Institute of Technology, Pasadena, CA, USA

Abstract Lightning is one of the most important sources of upper tropospheric NO_x; however, there is a large spread in estimates of the global emission rates (2–8 Tg N yr^{-1}). We combine upper tropospheric in situ observations from the Deep Convective Clouds and Chemistry (DC3) experiment and global satellite-retrieved NO_2 tropospheric column densities to constrain mean lightning NO_x (LNO_x) emissions per flash. Insights from DC3 indicate that the NO_x lifetime is ~3 h in the region of outflow of thunderstorms, mainly due to production of methyl peroxy nitrate and alkyl and multifunctional nitrates. The lifetime then increases farther downwind from the region of outflow. Reinterpreting previous analyses using the 3 h lifetime reduces the spread among various methods that have been used to calculate mean LNO_x emissions per flash and indicates a global LNO_x emission rate of ~9 Tg N yr^{-1}, a flux larger than the high end of recent estimates.

Plain Language Summary Lightning is an important source of upper troposphere nitrogen oxides; however, there is high uncertainty in the amount of nitrogen oxides produced from lightning. Using recent updates in upper tropospheric nitrogen oxides chemistry, this study decreases this uncertainty from a factor of 4 to less than a factor of 2 and shows that the amount of nitrogen oxides produced from lightning should be higher.

1. Introduction

In recent analyses, emissions of NO_x ($NO_x \equiv NO + NO_2$) from lightning have been estimated to be in the range of 2–8 Tg N yr^{-1}, representing ~10% of the global and ~80% of the middle to upper tropospheric NO_x source (Murray, 2016; Schumann & Huntrieser, 2007). Systematic variations in convectively available potential energy (CAPE), wind shear, and flash length have been suggested as mechanisms driving variability in emissions (Schumann & Huntrieser, 2007). However, observations have not established which of these mechanisms control mean lightning NO_x (LNO_x) emission rates per flash (Hudman et al., 2007; Martin et al., 2007; Schumann & Huntrieser, 2007). The LNO_x emission range can lead to at least a 15% difference in globally modeled tropospheric O_3, as estimated by Labrador et al. (2005), and up to a 60% increase in tropical O_3 (Liaskos et al., 2015).

Two methods are typically employed to estimate mean LNO_x emission rates per flash. The first method emphasizes the near field of convection and uses observations from either in situ or space-based platforms. These studies are typically based on the idea that the NO_x lifetime in the upper troposphere (UT) is long (2–8 days); using this assumption, the observations are directly converted to total NO_x emitted without an adjustment for chemical loss prior to measurement. The NO_x measurements are combined with the

number of lightning flashes observed in each of these individual events to yield the emission rate in units of mol NO flash^{-1} (Beirle et al., 2010, 2004; Bucsela et al., 2010; Huntrieser et al., 2007, 2009, 2011; Miyazaki et al., 2014; Pickering et al., 2016; Pollack et al., 2016). The second method uses in situ or space-based measurements in the far field to constrain a chemical transport model. The emission rate of NO from lightning is varied until the simulations broadly agree with measurements of NO_2, HNO_3, and/or NO_y (NO_y = NO + NO_2 + PAN + $CH_3O_2NO_2$ + HO_2NO_2 + alkyl and multifunctional nitrates + HNO_3 +…). Estimates of mol NO flash^{-1} are typically higher in far-field studies compared to near field, and both methods fail to accurately simulate the measured ratio of NO_x to HNO_3 (Allen et al., 2010, 2012; Fang et al., 2010; Hudman et al., 2007; Jourdain et al., 2010; Martini et al., 2011).

Here we largely resolve these conflicting interpretations of LNO_x. Recent improvements in our understanding of UT chemistry alter the relationships between near- and far-field concentrations of nitrogen oxides. We find that (1) the lifetime of NO_x in the near field of convection is much shorter than previously assumed (~2–3 h), reducing the downwind burden of NO_x relative to the magnitude of the emissions and, consequently, (2) that global LNO_x emissions are approximately 9 Tg N yr^{-1}—a value above the higher end of recent estimates.

2. Methods

We briefly describe the model and observations used in this study, and further details about the model and observations can be found in the supporting information.

Airborne observations from the Deep Convective Clouds and Chemistry (DC3) experiment were used in the analysis (Archive, 2014; Barth et al., 2015). Briefly, the NASA DC-8 aircraft sampled fresh and chemically aged LNO_x emissions over the continental United States, between May and June 2012. The details of the observations from the NASA DC-8 aircraft observations are described in the supporting information and include NO, NO_2, methyl peroxy nitrate ($CH_3O_2NO_2$), alkyl and multifunctional nitrates, HNO_3, O_3, and water vapor (Crounse et al., 2006; Day et al., 2002; Diskin et al., 2002; Nault et al., 2015; Ryerson et al., 1999; Talbot et al., 1997; Thornton et al., 2000). Descriptions of how the observations were filtered to match the chemical transport model can be found in the supporting information (Bertram et al., 2007; Cooper et al., 2014; Henderson et al., 2011; Hudman et al., 2007). Also, a discussion of the positive interference of thermally decomposed $CH_3O_2NO_2$ and pernitric acid on in situ UT NO_x observations from prior studies can be found in the supporting information (Browne et al., 2011; Nault et al., 2015).

The Ozone Monitoring Instrument (OMI) aboard the NASA Aura satellite is used to extend the observations, globally, for the year 2012 (Levelt et al., 2006). There are currently two products for global NO_2 column densities for OMI—the NASA Standard Product 2 (SP v2) (Bucsela et al., 2013) and the Dutch OMI NO_2 (DOMINO) Product (Boersma et al., 2011a, 2011b). For both, the Level 2 products were used to constrain LNO_x emissions around the world; the observations are matched to GEOS-Chem grid cells as described in the supporting information. Description of the air mass factor can be found in the supporting information (Boersma et al., 2002).

Finally, GEOS-Chem version 9-02 (http://geos-chem.org) (Bey et al., 2001) was used at 2° × 2.5° resolution. The standard chemistry, e.g., Sander et al. (2011), and model is described by Mao et al. (2013). Various changes to the chemical kinetics were analyzed (Table S1), and further details about GEOS-Chem can be found in the supporting information.

As a special note, we used the vertical distribution of LNO_x emissions recommended by Pickering et al. (1998). This profile was chosen since recent studies (Allen et al., 2012; Seltzer et al., 2015) conclude that the Ott et al. (2010) profile places too much NO_x in the middle troposphere and not enough NO_x in the UT.

3. Results

3.1. The Lifetime of NO_x

Our analysis begins by analyzing the impact of advances in our understanding of $CH_3O_2NO_2$ (Browne et al., 2011; Nault et al., 2015), HO_2NO_2 (Bacak et al., 2011; Nault et al., 2016), and dinitrogen pentoxide, N_2O_5 (Evans & Jacobs, 2005; Brown et al., 2009) and the reaction of OH with NO_2 to produce HNO_3 at the temperatures and pressures characteristic of convective outflow and the UT (Henderson et al., 2012; Nault et al., 2016) in the GEOS-Chem chemical transport model (Bey et al., 2001). Although, alkyl and multifunctional nitrates (ANs)

are known to play an important role in removing NO_x in the outflow of convective systems (Apel et al., 2012; Nault et al., 2016), no updates to AN chemistry were added because the impact of ANs is subgrid scale in this modeling framework. As discussed later, we evaluate the impact of neglecting their formation post hoc.

GEOS-Chem is used to calculate NO_x and HNO_3 mixing ratios and tropospheric NO_2 column densities ($tVCD_{NO2}$). Evaluations of the changes to the chemical kinetics individually (Figures S1–S3) show that $CH_3O_2NO_2$ chemistry creates an additional sink for NO_x, reducing the chemical lifetime of UT NO_x and reducing the $tVCD_{NO2}$ and the UT HNO_3. The effect of $CH_3O_2NO_2$ on NO_x concentrations and $tVCD_{NO2}$ is partly balanced by the revised low temperature and low-pressure rate of the reaction of NO_2 with OH, which results in an increase in the NO_x lifetime and, thus, higher NO_x concentrations and $tVCD_{NO2}$. This change to the low temperature HNO_3 source reinforces the effect of $CH_3O_2NO_2$ on UT HNO_3, as it also results in reduced HNO_3. The changes to HO_2NO_2 and N_2O_5 chemistry are included for completeness, but they had little effect on this analysis. Overall, even with the slower formation rate of HNO_3, the UT NO_x lifetime is reduced compared to the previously assumed 2–8 days (Schumann & Huntrieser, 2007).

These model results are consistent with observations, as further discussed in section 3.2. For example, in the near field, Nault et al. (2016) found that $CH_3O_2NO_2$ and ANs accounted for ~70% of the NO_x loss, whereas HNO_3 accounted for ~15% of the NO_x loss. Combining all the recent updates, the UT NO_x day time lifetime, inferred from the photostationary steady state described in Nault et al. (2016) and observations, is ~3 h near thunderstorms (i.e., < 6 h chemical aging) (Nault et al., 2016). After ~6 h chemical aging and dilution, the highly reactive hydrocarbons and HO_x precursors are reduced below other factors controlling the NO_x lifetime (Apel et al., 2012; Bertram et al., 2007; Fried et al., 2008), with the effect that the UT NO_x lifetime away from thunderstorms is ~0.5–1.5 days (Nault et al., 2016). Thus, LNO_x is rapidly lost to chemical removal in the near field of thunderstorms, but remnant NO_x plumes can still be observed up to 1–2 days after a storm (Figure S4).

3.2. Effects of Updated Chemistry on Interpretation of Near-Field Studies

Determination of the mol NO flash^{-1}, using near-field analyses of NO_x or NO_2 concentrations, requires that the loss of NO_x between emission and measurement be accounted for. These analyses typically assume that the UT NO_x lifetime is controlled by dilution and production of HNO_3 through the reaction of OH with NO_2, with values for the lifetime of NO_x in the range 2–8 days (Schumann & Huntrieser, 2007). We find that a much shorter lifetime, ~2–3 h, is consistent with in situ observations and the revised model (Nault et al., 2016). As a result, much more NO_x is likely being converted to higher oxides between emission and measurement than was previously recognized, leading to underestimation of the mol NO flash^{-1}.

Prior to applying this analysis to previous studies, we investigate the impact of the thermal decomposition of $CH_3O_2NO_2$ and HO_2NO_2 on near-field, in situ LNO_x measurements. We evaluate the maximum bias to NO_x from the thermal decomposition of these species during in situ sampling, using observations from the DC3 21 June 2012 flight. The chemical evolution of the near-field LNO_x emissions observed during this flight has been discussed in detail by Nault et al. (2016). For the UC Berkeley instrument and instruments with similar inlet design and exposure to warm cabin temperatures before measurement, at maximum, 5% of HO_2NO_2 would thermally decompose (Nault et al., 2015), leading to a positive bias of 3 parts per trillion by volume (pptv) in NO_2 and less than 1% bias in NO_x; thus, this compound is ignored for this discussion. In contrast, we assume full decomposition of $CH_3O_2NO_2$, as this molecule rapidly and completely dissociates to NO_2 and $CH_3O_2^{\cdot}$. Figure 1a shows that the thermal decomposition of $CH_3O_2NO_2$ would lead to an average ~ 7% positive bias in NO_x for the 21 June flight.

To demonstrate the impact of the shorter lifetime, we apply a post hoc correction to previous studies around the globe (Huntrieser et al., 2009; Schumann & Huntrieser, 2007). We assume that first-order kinetics (equation (1)) apply to the chemical conversion of lightning-emitted NO_x to higher oxides. We use this equation to extrapolate the moles of NO emitted at time $t = 0$, the time the lightning flashes were recorded, by the lightning flash from the measurement downwind at time t. The lifetime, τ, inferred from GEOS-Chem and observations by Nault et al. (2016) of ~3 h is used to solve for the initial value of emissions.

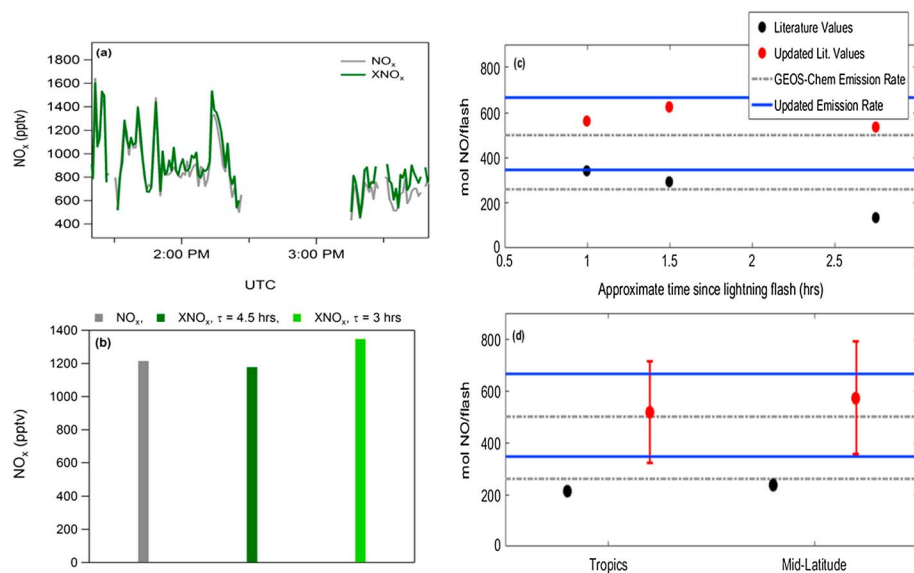$$\text{mol NO flash}^{-1}(t) = \text{mol NO flash}^{-1}(0) \times e^{-t/\tau} \tag{1}$$

Figure 1. (a) Time series of NO_x (grey) and XNO_x (NO_x + $CH_3O_2NO_2$, green) during DC3 21 June 2012 flight. (b) Average calculated NO_x (grey) and XNO_x (NO_x + $CH_3O_2NO_2$, both green) at $t = 0$ at 1:35 PM using equation (1). The difference between dark green and light green is assuming $\tau = 4.5$ h (accounting for $CH_3O_2NO_2$ interference) and $\tau = 3$ h (not accounting for $CH_3O_2NO_2$ interference). (c) Mol NO flash^{-1} calculated by Huntrieser et al. (2009) (black) using an assumed lifetime of ~2 days. The mol NO flash^{-1} (red) corresponds to the measured values calculated using a 3 h UT NO_x chemical lifetime. (d) The median tropical and midlatitude mol NO flash^{-1} (Huntrieser et al., 2009; Schumann & Huntrieser, 2007). The values calculated using an assumed ~ 2 day lifetime (black) and a 3 h chemical UT NO_x lifetime (red), and the error bars represent the range of time between emission and measurements from prior studies used to calculate the median mol NO flash^{-1} (Huntrieser et al., 2009; Schumann & Huntrieser, 2007). Error bars for the uncorrected values in Figure 1d are not shown, as they are less than 5 mol NO flash^{-1} when assuming a 2 day lifetime. For both Figures 1c and 1d, the dash dotted lines mark the tropical (260 mol NO flash^{-1}) and midlatitude (500 mol NO flash^{-1}) values used in the standard GEOS-Chem model and the solid blue lines are the values we recommend from this study.

Applying equation (1) to the DC3 flight from 21 June 2012, the average NO_x calculated for $t = 0$ is ~1200 pptv (Figure 1b). For other prior studies that measured in situ NO_2 along with NO, instead of calculating photostationary steady state NO_2, the apparent lifetime of NO_x could increase from 3 h to ~4.5 h if decomposed $CH_3O_2NO_2$ is not subtracted after measuring NO_2. This increase in apparent NO_x lifetime is due to measuring a NO_x sink, $CH_3O_2NO_2$, as NO_2 and $CH_3O_2NO_2$ accounts for ~50% of the NO_x loss during the 21st June flight. For this flight, if $CH_3O_2NO_2$ was measured as NO_2, but a 3 h lifetime is still assumed, the $t = 0$ NO_x is ~1350 pptv, ~13% too high (Figure 1b). Assuming a 4.5 h lifetime instead, to account for the inclusion of $CH_3O_2NO_2$ in the measurement, gives a $t = 0$ NO_x nearly identical to the case where only NO_x, and not $CH_3O_2NO_2 + NO_x$, is measured (Figure 1b). However, most studies, including the ones that are corrected post hoc here (Huntrieser et al., 2007, 2009, 2011; Schumann & Huntrieser, 2007), use NO measurements, which do not exhibit interference from $CH_3O_2NO_2$, and calculate the NO_2 mixing ratios; thus, we use the 3 h lifetime for the following analysis.

These prior studies, reviewed by Schumann and Huntrieser (2007), using a 2–8 day lifetime, report an average value of 250 mol NO flash^{-1} but with a significant range of values, including some as low as 20 mol flash^{-1}. If we reinterpret these studies' observations, using equation (1) with a 3 h chemical lifetime, the emission rate derived is approximately independent of time between lightning and the observation of the associated NO_x (Figures 1c–1d) and is more consistent with methods using far-field observations to constrain models. Emission rates derived from this revised analysis are in the range of 510 and 550 mol NO flash^{-1}, for tropics and midlatitudes, respectively (Figure 1d and Table S4). This is approximately a factor of 2 increase in values normally determined for mean LNO_x emission rates per flash determined in the near field of thunderstorms (Table S4) (Schumann & Huntrieser, 2007). This reduces the occurrence of very low mol NO flash^{-1} values, and thus the spread in global LNO_x emission estimates, as the lower bound of 2 Tg N yr^{-1} is mainly derived from these near-field analyses. Given the spread and uncertainty in the time since LNO_x emissions in the various
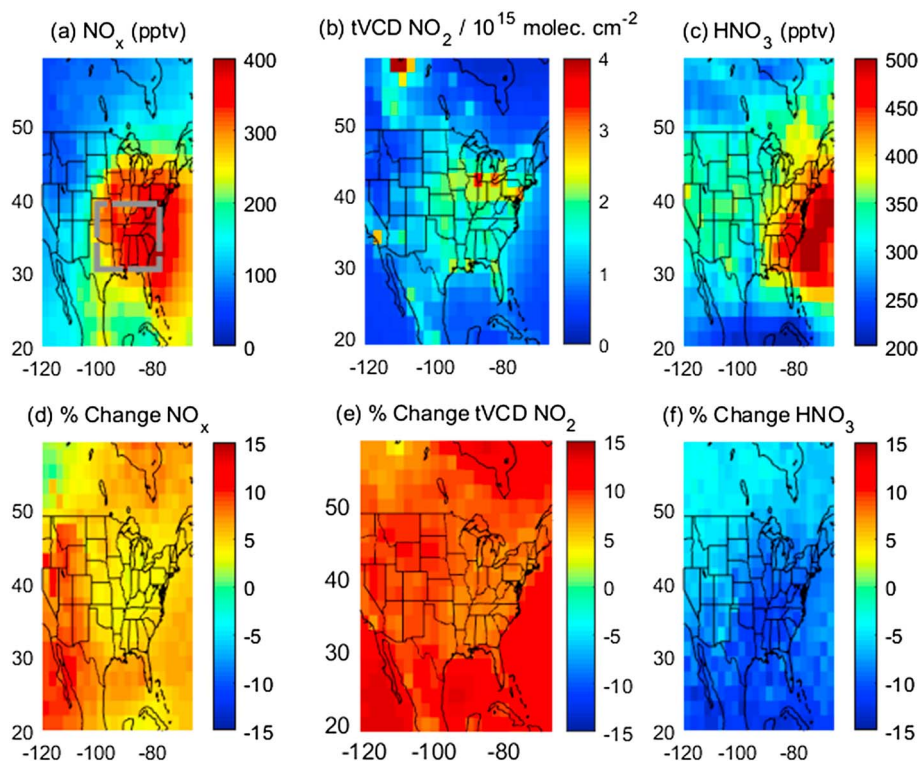
Figure 2. All results are from the simulations. Base case (a) UT NO_x, (b) tropospheric NO_2 column density (tVCD NO_2), and (c) UT HNO_3, where UT is defined as 200–350 hPa (defined in Table S1) between May and June 2012. Percent changes (updated chemistry - base)/updated chemistry (d) UT NO_x, (e) tVCD NO_2, and (f) UT HNO_3. The tVCD$_{NO2}$ is averaged between 12:00 and 14:00 local time, and the UT NO_x and HNO_3 are averaged between 16:00 and 20:00 local time. Grey box in Figure 2a highlights the region with high LNO$_x$ emissions.

studies, as indicated by the uncertainty in Figure 1d, the emission rate may be even higher (as high as 800 mol NO flash^{-1}).

3.3. Effects of Updated Chemistry on Interpretation of Far-Field Studies

Prior studies (Allen et al., 2010, 2012; Fang et al., 2010; Hudman et al., 2007; Martin et al., 2007; Martini et al., 2011), focusing on far-field concentrations, have recognized that it is difficult to simultaneously match both UT NO_x and HNO_3 observations. These studies chose an optimal value of 500 mol NO flash^{-1} for mean LNO$_x$ per flash (Table S4), which yields model concentrations at the lower end of the observed NO_x and the upper end of the observed HNO_3 (Figure S5).

In the southeastern United States (Figure 2), the region of the model most strongly affected by lightning (Hudman et al., 2007), our revised model has 11% lower UT HNO_3 mixing ratios than the base case, while the UT NO_x mixing ratios and tVCD$_{NO2}$ increase by 5% and 10%, respectively. With the revised chemistry (Figures 3 and S6), we find that increasing the mean LNO$_x$ emissions per flash by 33% to 665 mol NO flash^{-1} in the model leads to better agreement between the modeled and measured NO_x and similar agreement to HNO_3 as in prior studies. We find that UT HNO_3 observations are now predicted to be 54% higher than the observations, while NO_x is predicted to be within 10% of in situ.

Using this analysis in the southeast U.S., where we have in situ observations as a base for optimizing the model, we then compare to the global products available for OMI, the NASA SP v2 and the KNMI DOMINO product. Our model-satellite comparisons make use of averaging kernels (Boersma et al., 2016; Eskes & Boersma, 2003), so the comparisons are insensitive to the choice of a priori profiles in the retrieval. While a number of studies validating OMI tVCD$_{NO2}$ products using aircraft- or ground-based measurements or models have been done (Bucsela et al., 2008; Hains et al., 2010; Ialongo et al., 2016; Lamsal et al., 2010, 2014; Oetjen et al., 2013; Russell et al., 2011), they have mixed results on which product is more accurate, and no
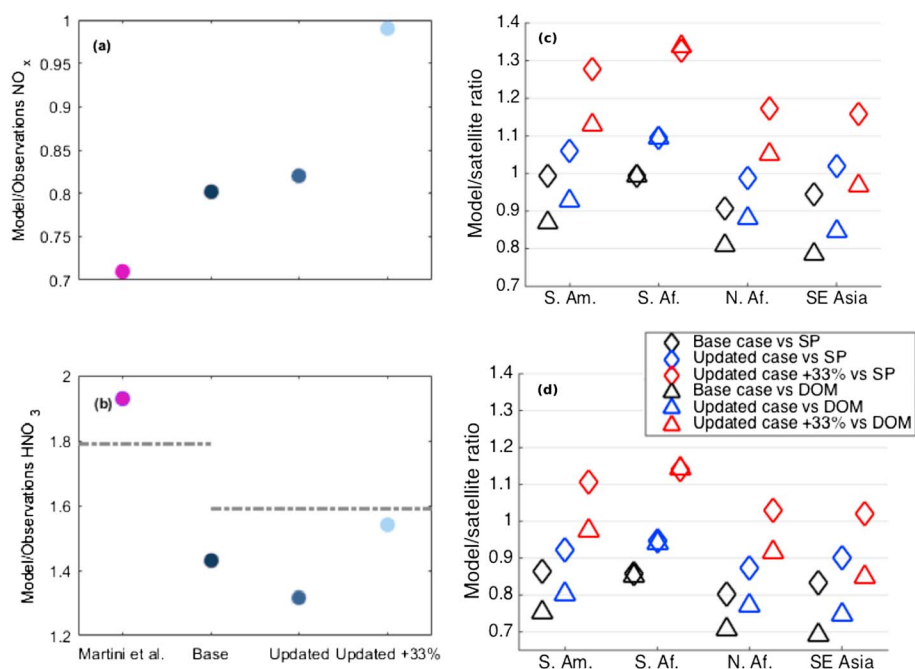
Figure 3. (a) Ratio of modeled and observed UT NO$_x$ from Martini et al. (2011), base case, updated chemistry case, and updated chemistry with +33% LNO$_x$ case (Table S1). (b) Ratio of modeled and observed UT HNO$_3$ from Martini et al. (2011), base case, updated case, and updated +33% case. Dash-dotted line represents the upper 1σ limit of observations in Martini et al. (2011) or during DC3. The NO$_x$ and HNO$_3$ observations from Martini et al. (2011) have been corrected for thermal decomposition of CH$_3$O$_2$NO$_2$ and HO$_2$NO$_2$, as suggested by Bertram et al. (2007) and Browne et al. (2011). The comparison with observations for the base, updated, and updated +33% case is from DC3. (c) Comparison of tropospheric NO$_2$ column density versus base case (black), updated case (blue), and updated +33% case (red) for South America (S. Am.), Southern Africa (S. Af.), Northern Africa (N. Af), and Southeast Asia (SE Asia). Diamonds and triangles are the NASA SPv2 (Bucsela et al., 2013) (SP) and DOMINOv2 (Boersma et al., 2011b) (DOM) NO$_2$ retrievals, respectively. The regions and time periods are defined in Table S2. The different cases are defined in Table S1. (d) As in Figure 3c but with GEOS-Chem profiles adjusted to NO$_2$:NO$_x$ ratios observed during DC3.

single study evaluates the versions of both the SP and DOMINO product used in this work; therefore, we use both products. The NASA SPv3 based on the revised slant columns described in Marchenko et al. (2015) was released after this analysis was completed. Krotkov et al. (2017) indicates that estimates of lightning NO$_x$ production efficiency will not change significantly with the new product.

Figure 3c shows that, in a direct comparison, the updated chemistry improves model-satellite agreement in three of four regions, although the +33% emission increase worsens the agreement in all regions. Previous studies (e.g., Travis et al., 2016) have identified differences between modeled and observed NO$_2$:NO$_x$ ratios in the UT. We therefore adjust the GEOS-Chem profiles to the average NO$_2$:NO$_x$ ratio observed during DC3 (Figure S7) for Figure 3d; with this, the two retrievals bracket a model/satellite ratio of one in three of four regions. In general, the satellite data support a 33% increase in lightning NO$_x$ emissions, especially in the Northern Hemisphere, though a smaller increase in the Southern Hemisphere may be indicated. This highlights the importance of further investigation into regionally specific lightning emissions. Assuming similar NO$_2$:NO$_x$ ratios in all regions, satellite-model comparisons support an annual production of 8.3–9.0 Tg N yr^{-1} from lightning; the lower value assumes the increase only in the Northern Hemisphere, the upper one globally.

The prior results were for grid-scale chemistry, and as previously mentioned, AN chemistry is subgrid. We take this chemistry into consideration, here, post hoc. Nault et al. (2016) observed ~40 pptv of ANs produced ~2 h downwind from deep convection; GEOS-Chem captures ~10 pptv of this production. We apply a post hoc correction here by removing 30 pptv from the modeled NO$_x$ and HNO$_3$ concentrations in pixels affected by lightning to represent possible repartitioning to ANs. We find that this post hoc correction, to the

updated chemistry case (without adjusting the lightning emissions), decreases NO_x, resulting in concentrations that are ~30% lower than DC3 observations and HNO_3 that is within 20% of DC3 observations (Figure S6). Applying this correction to the updated chemistry case with increased lighting emissions, we find that NO_x is ~10% lower than observations, while HNO_3 is still within the 1σ spread of the observations. Thus, if this estimate of the effect of ANs chemistry is representative of regional phenomena, then an additional 5–10% increase in emissions to at least 700 mol NO flash^{-1} would be required to yield modeled NO_x concentrations within 5% of DC3 observations.

4. Discussion

We identify that the UT NO_x lifetime near lightning is a key aspect contributing to current discrepancies between the near- and far-field studies of mean LNO_x emission rates per flash and a major contributor to the factor of 4 range in the emission rates that has been observed using different methods of data analysis (Schumann & Huntrieser, 2007). As demonstrated in Figure 1, once the UT NO_x lifetime is accounted for, two different approaches produce similar results for the mol NO flash^{-1}. After reevaluating the mean LNO_x emission rates per flash for the near-field studies and assuming 44 lightning flashes per second (Huntrieser et al., 2009), this would lead to ~9–10 Tg N yr^{-1}, which is similar to the total value calculated in the updated GEOS-Chem model run constrained by far-field studies (Table S4), assuming a global increase. This demonstrates that both the greater mol flash^{-1} and the updated chemistry are necessary to optimize the agreement between models and observations. Additionally, this reduced spread in emission rates should greatly decrease the current differences among models and between models and measurements (Table S4).

Measurements of NO_y can also be utilized to circumvent the rapid UT NO_x chemistry to determine lightning N emission rate. In the near field of LNO_x emissions, NO_x is a large fraction of the total NO_y budget—up to 70–80% (Huntrieser et al., 2009, 2011). As NO_x rapidly oxidizes, total NO_y remains conserved, meaning that a measurement of total NO_y would provide a more useful constraint for lightning N emissions without needing prior knowledge or calculations of the NO_x chemistry and lifetime. For example, Nault et al. (2016) observed nearly complete closure between the rapid loss of NO_x (2.6×10^5 molecules/cm^3/s) and production of its higher oxide species (2.3×10^5 molecules/cm^3/s), demonstrating both the aforementioned rapid loss of NO_x in the first 3 h downwind from LNO_x emissions (as discussed throughout this paper) and the conservation of NO_y. Using the NO_y measurements in these two studies, we calculate 400 (Huntrieser et al., 2009) and 479 (Huntrieser et al., 2011) NO mol flash^{-1}. This would correspond to 7–9 Tg N yr^{-1} from lightning. This further indicates that the mean LNO_x emission rates per flash have been underpredicted and NO_y, when available, is a better measurement to calculate mean LNO_x emission rates per flash. However, measurement of total NO_y cannot be achieved from space-based platforms; therefore, accurate knowledge of the partitioning of NO_x to its higher oxides remains important for space-based near-field studies.

Another compound impacted by the increased LNO_x emission rates is UT O_3, an important greenhouse gas (Myre et al., 2013). The increased LNO_x emissions increase modeled UT O_3, which increases the differences between observed and modeled UT O_3 (Figure S8). Though investigating all the mechanisms that lead to this discrepancy between model and observations is beyond the scope of this paper, we speculate that the bias is due to subgrid effects of water vapor transport (Sauvage et al., 2007). The modeled water vapor mixing ratios are higher (by as much as 100%) than observed during DC3 (Figure S9). Since water is a key term in O_3 production, correcting this bias would likely improve the representation of UT O_3.

5. Conclusions

Utilizing the recent updates, including rapid $CH_3O_2NO_2$ and ANs production, in UT NO_x lifetime and fate improves our understanding of mean lightning NO_x (LNO_x) emission rates per flash. Incorporating these updates into a global chemical transport model, we find that the mean LNO_x emission rates per flash should increase by 23–33% to better match in situ measurements of NO_x and HNO_3 and satellite measurements of $tVCD_{NO2}$. The increase in inferred emissions stems from (a) the updated chemistry that decreases UT HNO_3, preventing the prior model overestimate of UT HNO_3 from limiting mean LNO_x emission rates per flash, and (b) from using a consistent, short NO_x lifetime instead of the one assumed in prior studies. This reduces the discrepancy of LNO_x among previous analyses.

References

Allen, D., Pickering, K., Duncan, B., & Damon, M. (2010). Impact of lightning NO emissions on North American photochemistry as determined using the Global Modeling Initiative (GMI) model. *Journal of Geophysical Research*, *115*, D22301. https://doi.org/10.1029/2010JD014062

Allen, D. J., Pickering, K. E., Pinder, R. W., Henderson, B. H., Appel, K. W., & Prados, A. (2012). Impact of lightning-NO on eastern United States photochemistry during the summer of 2006 as determined using the CMAQ model. *Atmospheric Chemistry and Physics*, *12*(4), 1737–1758. https://doi.org/10.5194/acp-12-1737-2012

Apel, E. C., Olson, J. R., Crawford, J. H., Hornbrook, R. S., Hills, A. J., Cantrell, C. A., … Riemer, D. D. (2012). Impact of the deep convection of isoprene and other reactive trace species on radicals and ozone in the upper troposphere. *Atmospheric Chemistry and Physics*, *12*(2), 1135–1150. https://doi.org/10.5194/acp-12-1135-2012

Archive, National aeronautical and space agency, deep convective clouds and chemistry, DC-8, Version 5, 2014(September 20). Available from: https://doi.org/10.5067/Aircraft/DC3/DC8/Aerosol-TraceGas

Bacak, A., Cookeb, M. C., Bardwella, M. W., McGillena, M. R., Archibaldbc, A. T., Hueyd, L. G., … Percivala, C. J. (2011). Kinetics of the $HO_2 + NO_2$ Reaction: On the impact of new gas-phase kinetic data for the formation of HO_2NO_2 on HO_x, NO_x and HO_2NO_2 levels in the troposphere. *Atmospheric Environment*, *45*(35), 6414–6422. https://doi.org/10.1016/j.atmosenv.2011.08.008

Barth, M. C., Cantrell, C. A., Brune, W. H., Rutledge, S. A., Crawford, J. H., Huntrieser, H., … Ziegler, C. (2015). The Deep Convective Clouds and Chemistry (DC3) Field Campaign. *Bulletin of the American Meteorological Society*, *96*(8), 1281–1309. https://doi.org/10.1175/BAMS-D-13-00290.1

Beirle, S., Platt, U., Wenig, M., & Wagner, T. (2004). NO_x production by lightning estimated with GOME, edited by J. P. T. Burrows AM. *Advances in Space Research*, *34*(4), 793–797. https://doi.org/10.1016/j.asr.2003.07.069

Beirle, S., Huntrieser, H., & Wagner, T. (2010). Direct satellite observation of lightning-produced NO_x. *Atmospheric Chemistry and Physics*, *10*(22), 10965–10986. https://doi.org/10.5194/acp-10-10965-2010

Bertram, T. H., Perring, A. E., Wooldridge, P. J., Crounse, J. D., Kwan, A. J., Wennberg, P. O., … Cohen, R. C. (2007). Direct measurements of the convective recycling of the upper troposphere. *Science*, *315*(5813), 816–820. https://doi.org/10.1126/science.1134548

Bey, I., Jacob, D. J., Yantosca, R. M., Logan, J. A., Field, B. D., Fiore, A. M., … Schultz, M. G. (2001). Global modeling of tropospheric chemistry with assimilated meteorology: Model description and evaluation. *Journal of Geophysical Research*, *106*(D19), 23073–23095. https://doi.org/10.1029/2001JD000807

Boersma, K. F., Bucsela, E. J., Brinksma, E. J., & Gleason, J. F. (2002). NO2, OMI Algorithm Theor. Basis Doc. Vol. 4, Omi Trace Gas Algorithms, *ATB-OMI-04, version 2.0*, 13–36. Available from: http://eospso.nasa.gov/sites/default/files/atbd/ ATBD-OMI-04.pdf (Accessed 22 November 2016).

Boersma, K. F., Braak, R., & van der A, R. J. (2011a). Dutch OMI NO2 (DOMINO) data product 2.0 HE5 data file user manual, p. 17. Available from http://www.temis.nl/docs/OMI_NO2_HE5_2.0_2011.pdf (Accessed 25 Aug 2017).

Boersma, K. F., Eskes, H. J., Dirksen, R. J., van der A, R. J., Veefkind, J. P., Stammes, P., … Brunner, D. (2011b). An improved tropospheric NO_2 column retrieval algorithm for the Ozone Monitoring Instrument. *Atmospheric Measurement Techniques*, *4*(9), 1905–1928. https://doi.org/10.5194/amt-4-1905-2011

Boersma, K. F., Vinken, G. C. M., & Eskes, H. J. (2016). Representativeness errors in comparing chemistry transport and chemistry climate models with satellite UV–Vis tropospheric column retrievals. *Geoscientific Model Development*, *9*(2), 875–898. https://doi.org/10.5194/gmd-9-875-2016

Brown, S. S., Dube, W. P., Fuchs, H., Ryerson, T. B., Wollny, A. G., Brock, C. A., … Ravishankara, A. R. (2009). Reactive uptake coefficients for N_2O_5 determined from aircraft measurements during the Second Texas Air Quality Study: Comparison to current model parameterizations. *Journal of Geophysical Research*, *114*, D00F10. https://doi.org/10.1029/2008JD011679

Browne, E. C., Perring, A. E., Wooldridge, P. J., Apel, E., Hall, S. R., Huey, L. G., … Cohen, R. C. (2011). Global and regional effects of the photochemistry of $CH_3O_2NO_2$: Evidence from ARCTAS. *Atmospheric Chemistry and Physics*, *11*(9), 4209–4219. https://doi.org/10.5194/acp-11-4209-2011

Bucsela, E. J., Perring, A. E., Cohen, R. C., Boersma, K. F., Celarier, E. A., Gleason, J. F., … Veefkind, J. P. (2008). Comparison of tropospheric NO_2 from in situ aircraft measurements with near-real-time and standard product data from OMI. *Journal of Geophysical Research*, *113*, D16S31. https://doi.org/10.1029/2007JD008838

Bucsela, E. J., Pickering, K. E., Huntemann, T. L., Cohen, R. C., Perring, A., Gleason, J. F., … Laporte-Molina, S. (2010). Lightning-generated NO_x seen by the Ozone Monitoring Instrument during NASA's Tropical Composition, Cloud and Climate Coupling Experiment (TC4). *Journal of Geophysical Research*, *115*, D00J10. https://doi.org/10.1029/2009JD013118

Bucsela, E. J., Krotkov, N. A., Celarier, E. A., Lamsal, L. N., Swartz, W. H., Bhartia, P. K., … Pickering, K. E. (2013). A new stratospheric and tropospheric NO_2 retrieval algorithm for nadir-viewing satellite instruments: Applications to OMI. *Atmospheric Measurement Techniques*, *6*(10), 2607–2626. https://doi.org/10.5194/amt-6-2607-2013

Cooper, M., Martin, R. V., Wespes, C., Coheur, P.-F., Clerbaux, C., & Murray, L. T. (2014). Tropospheric nitric acid columns from the IASI satellite instrument interpreted with a chemical transport model: Implications for parameterizations of nitric oxide production by lightning. *Journal of Geophysical Research: Atmospheres*, *119*, 10068–10079. https://doi.org/10.1002/2014JD021907

Crounse, J. D., McKinney, K. A., Kwan, A. J., & Wennberg, P. O. (2006). Measurement of Gas-Phase Hydroperoxides by Chemical Ionization Mass Spectrometry. *Analytical Chemistry*, *78*(19), 6726–6732. https://doi.org/10.1021/ac0604235

Day, D. A., Wooldridge, P. J., Dillon, M. B., Thornton, J. A., & Cohen, R. C. (2002). A thermal dissociation laser-induced fluorescence instrument for in situ detection of NO_2, peroxy nitrates, alkyl nitrates, and HNO_3. *Journal of Geophysical Research*, *107*(D5–6), 4046. https://doi.org/10.1029/2001JD000779

Diskin, G. S., Podolske, J. R., Sachse, G. W., & Slate, T. A. (2002). Open-path airborne tunable diode laser hygrometer, in: Diode Lasers and Applications in Atmospheric Sensing, edited by: Fried, A. *Proceeding of the Society Photo-Optical Instrumentation Engineering*, *4817*, 196–204. https://doi.org/10.1117/12.453736

Eskes, H. J., & Boersma, K. F. (2003). Averaging kernels for DOAS total-column satellite retrievals. *Atmospheric Chemistry and Physics*, *3*(5), 1285–1291. https://doi.org/10.5194/acp-3-1285-2003

Evans, M. J., & Jacob, D. J. (2005). Impact of new laboratory studies of N_2O_5 hydrolysis on global model budgets of tropospheric nitrogen oxides, ozone, and OH. *Geophysical Research Letters*, *32*, L09813. https://doi.org/10.1029/2005GL022469

Fang, Y., Fiore, A. M., Horowitz, L. W., Levy, H. II, Hu, Y., & Russell, A. G. (2010). Sensitivity of the NO_y budget over the United States to anthropogenic and lightning NO_x in summer. *Journal of Geophysical Research*, *115*, D18312. https://doi.org/10.1029/2010JD014079

Fried, A., Olson, J. R., Walega, J. G., Crawford, J. H., Chen, G., Weibring, P., … Millet, D. B. (2008). Role of convection in redistributing formaldehyde to the upper troposphere over North America and the North Atlantic during the summer 2004 INTEX campaign. *Journal of Geophysical Research*, *113*, D17306. https://doi.org/10.1029/2007JD009760

Hains, J. C., Boersma, K. F., Kroon, M., Dirksen, R. J., Cohen, R. C., Perring, A. E., … Levelt, P. (2010). Testing and improving OMI DOMINO tropospheric NO_2 using observations from the DANDELIONS and INTEX-B validation campaigns. *Journal of Geophysical Research*, *115*, D05301. https://doi.org/10.1029/2009JD012399

Henderson, B. H., Pinder, R. W., Crooks, J., Cohen, R. C., Hutzell, W. T., Sarwar, G., … Vizuete, W. (2011). Evaluation of simulated photochemical partitioning of oxidized nitrogen in the upper troposphere. *Atmospheric Chemistry and Physics*, *11*(1), 275–291. https://doi.org/10.5194/acp-11-275-2011

Henderson, B. H., Pinder, R. W., Crooks, J., Cohen, R. C., Carlton, A. G., Pye, H. O. T., & Vizuete, W. (2012). Combining Bayesian methods and aircraft observations to constrain the $HO^·$ + NO_2 reaction rate. *Atmospheric Chemistry and Physics*, *12*(2), 653–667. https://doi.org/10.5194/acp-12-653-2012

Hudman, R. C., Jacob, D. J., Turquety, S., Leibensperger, E. M., Murray, L. T., Wu, S., … Wooldridge, P. J. (2007). Surface and lightning sources of nitrogen oxides over the United States: Magnitudes, chemical evolution, and outflow. *Journal of Geophysical Research*, *112*, D12S05. https://doi.org/10.1029/2006JD007912

Huntrieser, H., Schlager, H., Roiger, A., Lichtenstern, M., Schumann, U., Kurz, C., … Stohl, A. (2007). Lightning-produced NO_x over Brazil during TROCCINOX: Airborne measurements in tropical and subtropical thunderstorms and the importance of mesoscale convective systems. *Atmospheric Chemistry and Physics*, *7*(11), 2987–3013. https://doi.org/10.5194/acp-7-2987-2007

Huntrieser, H., Schlager, H., Lichtenstern, M., Roiger, A., Stock, P., Minikin, A., … Brunner, D. (2009). NO_x production by lightning in Hector: First airborne measurements during SCOUT-O3/ACTIVE. *Atmospheric Chemistry and Physics*, *9*(21), 8377–8412. https://doi.org/10.5194/acp-9-8377-2009

Huntrieser, H., Schlager, H., Lichtenstern, M., Stock, P., Hamburger, T., Hoeller, H., … Ravegnani, F. (2011). Mesoscale convective systems observed during AMMA and their impact on the NO_x and O_3 budget over West Africa. *Atmospheric Chemistry and Physics*, *11*(6), 2503–2536. https://doi.org/10.5194/acp-11-2503-2011

Ialongo, I., Herman, J., Krotkov, N., Lamsal, L., Boersma, K. F., Hovila, J., & Tamminen, J. (2016). Comparison of OMI NO_2 observations and their seasonal and weekly cycles with ground-based measurements in Helsinki. *Atmospheric Measurement Techniques*, *9*(10), 5203–5212. https://doi.org/10.5194/amt-9-5203-2016

Jourdain, L., Kulawik, S. S., Worden, H. M., Pickering, K. E., Worden, J., & Thompson, A. M. (2010). Lightning NO_x emissions over the USA constrained by TES ozone observations and the GEOS-Chem model. *Atmospheric Chemistry and Physics*, *10*(1), 107–119. https://doi.org/10.5194/acp-10-107-2010

Krotkov, N. A., Lamsal, L. N., Celarier, E. A., Swartz, W. H., Marchenko, S. V., Bucsela, E. J., … Zara, M. (2017). The version 3 OMI NO_2 standard product, *Atmospheric Measurement Techniques*, *10*, 3133–3149. https://doi.org/10.5194/amt-10-3133-2017

Labrador, L. J., von Kuhlmann, R., & Lawrence, M. G. (2005). The effects of lightning-produced NO_x and its vertical distribution on atmospheric chemistry: Sensitivity simulations with MATCH-MPIC. *Atmospheric Chemistry and Physics*, *5*, 1815–1834. https://doi.org/10.5194/acp-5-1815-2005

Lamsal, L. N., Martin, R. V., Van Donkelaar, A., Celarier, E. A., Bucsela, E. J., Boersma, K. F., … Wang, Y. (2010). Indirect validation of tropospheric nitrogen dioxide retrieved from the OMI satellite instrument: Insight into the seasonal variation of nitrogen oxides at northern midlatitudes. *Journal of Geophysical Research*, *115*, D05302. https://doi.org/10.1029/2009JD013351

Lamsal, L. N., Krotkov, N. A., Celarier, E. A., Swartz, W. H., Pickering, K. E., Bucsela, E. J., … Knepp, T. N. (2014). Evaluation of OMI operational standard NO_2 column retrievals using in situ and surface-based NO_2 observations. *Atmospheric Chemistry and Physics*, *14*(21), 11587–11609. https://doi.org/10.5194/acp-14-11587-2014

Levelt, P. F., Van den Oord, G. H. J., Dobber, M. R., Malkki, A., Visser, H., de Vries, J., … Saari, H. (2006). The Ozone Monitoring Instrument. *IEEE Transactions on Geoscience and Remote Sensing*, *44*(5), 1093–1101. https://doi.org/10.1109/TGRS.2006.872333

Liaskos, C. E., Allen, D. J., & Pickering, K. E. (2015). Sensitivity of tropical tropospheric composition to lightning NO_x production as determined by replay simulations with GEOS-5. *Journal of Geophysical Research: Atmospheres*, *120*, 8512–8534. https://doi.org/10.1002/2014JD022987

Mao, J., Paulot, F., Jacob, D. J., Cohen, R. C., Crounse, J. D., Wennberg, P. O., … Horowitz, L. W. (2013). Ozone and organic nitrates over the eastern United States: Sensitivity to isoprene chemistry. *Journal of Geophysical Research: Atmospheres*, *118*, 11256–11268. https://doi.org/10.1002/jgrd.50817

Marchenko, S., Krotkov, N. A., Lamsal, L. N., Celarier, E. A., Swartz, W. H., & Bucsela, E. J. (2015). Revising the slant column density retrieval of nitrogen dioxide observed by the Ozone Monitoring Instrument. *Journal of Geophysical Research: Atmospheres*, *120*, 5670–5692. https://doi.org/10.1002/2014JD022913

Martin, R. V., Sauvage, B., Folkins, I., Sioris, C. E., Boone, C., Bernath, P., & Ziemke, J. (2007). Space-based constraints on the production of nitric oxide by lightning. *Journal of Geophysical Research*, *112*, D09309. https://doi.org/10.1029/2006JD007831

Martini, M., Allen, D. J., Pickering, K. E., Stenchikov, G. L., Richter, A., Hyer, E. J., & Loughner, C. P. (2011). The impact of North American anthropogenic emissions and lightning on long-range transport of trace gases and their export from the continent during summers 2002 and 2004. *Journal of Geophysical Research*, *116*, D07305. https://doi.org/10.1029/2010JD014305

Miyazaki, K., Eskes, H. J., Sudo, K., & Zhang, C. (2014). Global lightning NO_x production estimated by an assimilation of multiple satellite data sets. *Atmospheric Chemistry and Physics*, *14*(7), 3277–3305. https://doi.org/10.5194/acp-14-3277-2014

Murray, L. T. (2016). Lightning NO_x and impacts on air quality. *Currents Pollution Reports*, *2*(2), 115–133. https://doi.org/10.1007/s40726-016-0031-7

Myre, G., Shindell, D., Bréon, F.-M., Collins, W., Fuglestvedt, J., Huang, J., … Zhang, H. (2013). Anthropogenic and natural radiative forcing. In T. F. Stocker et al. (Eds.), *Climate Change 2013: The Physical Science Basis. Contribution of Working Group I to the Fifth Assessment Report of the Intergovernmental Panel on Climate Change* (pp. 659–740). Cambridge, United Kingdom and New York, NY, USA: Cambridge University Press.

Nault, B. A., Garland, C., Pusede, S. E., Wooldridge, P. J., Ullmann, K., Hall, S. R., & Cohen, R. C. (2015). Measurements of $CH_3O_2NO_2$ in the upper troposphere. *Atmospheric Measurement Techniques*, *8*(2), 987–997. https://doi.org/10.5194/amt-8-987-2015

Nault, B. A., Garland, C., Wooldridge, P. J., Brune, W. H., Campuzano-Jost, P., Crounse, J. D., … Cohen, R. C. (2016). Observational Constraints on the Oxidation of NO_x in the Upper Troposphere. *The Journal of Physical Chemistry. A*, *120*(9), 1468–1478. https://doi.org/10.1021/acs.jpca.5b07824

Oetjen, H., Baidar, S., Krotkov, N. A., Lamsal, L. N., Lechner, M., & Volkamer, R. (2013). Airborne MAX-DOAS measurements over California: Testing the NASA OMI tropospheric NO_2 product. *Journal of Geophysical Research: Atmospheres*, *118*, 7400–7413. https://doi.org/10.1002/jgrd.50550

Ott, L. E., Pickering, K. E., Stenchikov, G. L., Allen, D. J., DeCaria, A. J., Ridley, B., … Tao, W.-K. (2010). Production of lightning NO_x and its vertical distribution calculated from three-dimensional cloud-scale chemical transport model simulations. *Journal of Geophysical Research*, *115*, D04301. https://doi.org/10.1029/2009JD011880

Pickering, K. E., Wang, Y., Tao, W.-K., Price, C., & Müller, J.-F. (1998). Vertical distributions of lightning NO_x for use in regional and global chemical transport models. *Journal of Geophysical Research*, *103*(D23), 31203. https://doi.org/10.1029/98JD02651

Pickering, K. E., Bucsela, E., Allen, D., Ring, A., Holzworth, R., & Krotkov, N. (2016). Estimates of lightning NO_x production based on OMI NO_2 observations over the Gulf of Mexico. *Journal of Geophysical Research: Atmospheres*, *121*(14), 8668–8691. https://doi.org/10.1002/2015JD024179

Pollack, I. B., Homeyer, C. R., Ryerson, T. B., Aikin, K. C., Peischl, J., Apel, E. C., … Barth, M. C. (2016). Airborne quantification of upper tropospheric NO_x production from lightning in deep convective storms over the United States Great Plains. *Journal of Geophysical Research: Atmospheres*, *121*, 2002–2028. https://doi.org/10.1002/2015JD023941

Russell, A. R., Perring, A. E., Valin, L. C., Bucsela, E. J., Browne, E. C., Wooldridge, P. J., & Cohen, R. C. (2011). A high spatial resolution retrieval of NO_2 column densities from OMI: Method and evaluation. *Atmospheric Chemistry and Physics*, *11*(16), 8543–8554. https://doi.org/10.5194/acp-11-8543-2011

Ryerson, T. B., Huey, L. G., Knapp, K., Neuman, J. A., Parrish, D. D., Sueper, D. T., & Fehsenfeld, F. C. (1999). Design and initial characterization of an inlet for gas-phase NO_y measurements from aircraft. *Journal of Geophysical Research*, *104*(D5), 5483–5492. https://doi.org/10.1029/1998JD100087

Sander, S. P., Abbatt, J., Barker, J. R., Burkholder, J. B., Friedl, R. R., Golden, D. M. , … Wine, P. H. (2011). Chemical kinetics and photochemical data for use in atmospheric studies, Evaluation No. 17, JPL Publ. 10-6, Jet Propuls. Lab. Pasadena.

Sauvage, B., Martin, R. V., van Donkelaar, A., Liu, X., Chance, K., Jaeglé, L., … Fu, T.-M. (2007). Remote sensed and in situ constraints on processes affecting tropical tropospheric ozone. *Atmospheric Chemistry and Physics*, *7*(3), 815–838. https://doi.org/10.5194/acp-7-815-2007

Schumann, U., & Huntrieser, H. (2007). The global lightning-induced nitrogen oxides source. *Atmospheric Chemistry and Physics*, *7*(14), 3823–3907. https://doi.org/10.5194/acp-7-3823-2007

Seltzer, K. M., Vizuete, W., & Henderson, B. H. (2015). Evaluation of updated nitric acid chemistry on ozone precursors and radiative effects. *Atmospheric Chemistry and Physics*, *15*(10), 5973–5986. https://doi.org/10.5194/acp-15-5973-2015

Talbot, R. W., Dibb, J. E., Lefer, B. L., Scheuer, E. M., Bradshaw, J. D., Sandholm, S. T., … Gregory, G. L. (1997). Large-scale distributions of tropospheric nitric, formic, and acetic acids over the western Pacific basin during wintertime. *Journal of Geophysical Research*, *102*(D23), 28303–28313. https://doi.org/10.1029/96JD02975

Thornton, J. A., Wooldridge, P. J., & Cohen, R. C. (2000). Atmospheric NO_2: In-situ laser-induced fluorescence detection at parts per trillion mixing ratios. *Analytical Chemistry*, *72*(3), 528–539. https://doi.org/10.1021/ac9908905

Travis, K. R., Jacob, D. J., Fisher, J. A., Kim, P. S., Marais, E. A., Zhu, L., … Zhou, X. (2016). Why do models overestimate surface ozone in the Southeast United States?. *Atmospheric Chemistry and Physics*, *16*(21), 13561–13577. https://doi.org/10.5194/acp-16-13561-2016